LC-MS/MS metabolome analysis detects the changes in the lipid metabolic profiles of dMMR and pMMR cells

WEN PENG[1,2*], SHISHENG TAN[2*], YOUZHI XU[3*], LIANG WANG[4], DONG QIU[2], CHAN CHENG[2], YIYUN LIN[1], CHUNQI LIU[1], ZHUOLIN LI[1], YAN LI[1], YINGLAN ZHAO[1] and QIU LI[1]

[1]Department of Medical Oncology, Cancer Center, West China Hospital, Sichuan University, Chengdu, Sichuan 610041; [2]Department of Oncology, The People's Hospital of Guizhou Province, Guiyang, Guizhou 550004; [3]Department of Pathophysiology, School of Basic Medicine, Anhui Medical University, Hefei, Anhui 230032, P.R. China; [4]Institute of Biotechnology, University of Helsinki, 00014 Helsinki, Finland

Received November 29, 2017; Accepted June 8, 2018

DOI: 10.3892/or.2018.6510

Abstract. The DNA mismatch repair (MMR) system plays an important role in the initiation, diagnosis and treatments of colorectal cancer (CRC). Compared to CRC patients deficient in DNA MMR (dMMR), CRC patients proficient in DNA MMR (pMMR) have higher metastasis, short survival and poor response to chemotherapy and immunotherapy. It is well-known that a high-fat diet can cause CRC, and lipid metabolism is closely related to the development and metastasis of CRC. However, there have been few studies that address the difference in lipid metabolism between dMMR and pMMR CRC. Liquid chromatography-tandem mass spectrometry (LC/MS) is an advanced technique that can perform the analysis of lipid metabolites and the roles of lipids present in low abundance in cell signaling and membrane stability. In the present study, we used the LC/MS technique to analyze the difference in the lipid metabolic profiles between dMMR cell lines (HCT116, DLD1, LoVo and HCT15) and pMMR cell lines (SW480, SW620, HT29 and NCM460). The results revealed that, among the 19 classes and 157 intact lipid species identified by the LC/MS analysis, the levels of most phospholipids were lower in dMMR cells than pMMR cells. Higher levels of phosphatidylcholine (PC; 16:0/18:1) and phosphatidic acid (PA; 18:0/18:0) were observed in pMMR cells than in dMMR cells. Furthermore, our results revealed that SCD1 and PLD1, the key enzymes involved in lipid metabolism associated with metastasis, are higher in pMMR cells than dMMR cells. To the best of our knowledge, we are the first to reveal that the levels of metastasis-associated lipids and key enzymes in lipid metabolism were higher in the CRC patients with pMMR compared with the CRC patients with dMMR. This study identified potential anti-metastatic targets in the therapy of patients with pMMR, and also personalized therapy for the patients with pMMR.

Correspondence to: Dr Yinglan Zhao or Dr Qiu Li, Department of Medical Oncology, Cancer Center, West China Hospital, Sichuan University, 17 Renmin South Road 3rd Section, Chengdu, Sichuan 610041, P.R. China
E-mail: zhaoyinglan@scu.edu.cn
E-mail: fbqiu9@163.com

*Contributed equally

Key words: LC-MS, dMMR, pMMR, colorectal cancer, lipid metabolism

Introduction

Colorectal cancer (CRC) is ranked as the third most common cancer in males and second in females, and the fourth leading cause of cancer-related deaths worldwide (1). For the patients with early CRC, surgery is the preferred treatment, and adjuvant chemotherapy is administered to most patients with CRC after surgery to decrease the risk of recurrence (2). However, the disease-free and overall survival of CRC patients warrants further improvement. The elucidation of the molecular pathogenesis of CRC may greatly contribute to prolong the survival of CRC patients.

The DNA mismatch repair (MMR) system is important for the prevention of gene mutations and maintenance of genome stability (3). The MMR system includes the hMLH1, hMSH2, hMSH6, and hPSM2 genes, and defects of the MMR system are caused by deficient MMR genes (dMMR) in tumor suppressor genes such as APC and p53 which are closely related to tumorigenesis mutations (4). Approximately 12-15% of CRC patients display dMMR, whereas 80-90% of CRC patients exhibit pMMR (5). Compared with pMMR patients, dMMR patients have a low relapse rate, long remission period, low metastasis, high survival rate and good prognosis (6).

The mechanisms by which the MMR genes affect the pathogenesis of CRC may vary and involve not only important components of the internal organelles in cells but also important homeostasis processes, such as energy transfer, material transport, information identification and signal transduction, differentiation, apoptosis and immunity (7). Changes in enzymes involved in lipid metabolism and their pathways are related to the cancer type, staging, malignancy and therapeutic

efficacy (8). Accumulating evidence from basic studies suggests that the change of lipid levels is associated with human gene mutations that would influence the treatment and prognosis of cancer (9). It is well-known that a high-fat diet can easily cause CRC, and it has been reported that lipid metabolism is closely related to the initiation, development and metastasis of CRC (2). However, there have been few studies that address the difference in lipid metabolism between dMMR and pMMR CRC. The lack of reliable and precise lipid analysis technology severely hampers the analysis of the relationship between lipid metabolism and CRC.

Liquid chromatography-tandem mass spectrometry (LC/MS) allows the quantitative detection of hundreds of lipids in tumor cell membranes, an accurate analysis of lipid metabolites and the roles of lipids present in low abundance in cell signaling and membrane stability (10). Studies on lipid metabolism in CRC have revealed that the levels of phosphatidylethanolamine (PE), phosphatidylserine (PS) and phosphatidylcholine (PC) metabolites were significantly increased compared with polyps and healthy controls (11). In the present study, we used the LC/MS technique to analyze the difference in lipid metabolism between dMMR and pMMR CRC.

We hereby analyzed the lipid metabolic profiles of dMMR and pMMR CRC cells using reverse-phase liquid chromatography-quadrupole-time-of-flight mass spectrometry (Q-TOF/MS) comprehensively. The present study revealed that the levels of metastasis-associated lipids and key enzymes in lipid metabolism were revealed to be higher in the CRC patients with pMMR compared with the CRC patients with dMMR, and offered novel insights into potential therapeutic targets and individual treatment strategies for CRC patients with dMMR and pMMR.

Materials and methods

Cell culture. The human colon carcinoma cancer cell lines SW620, SW480, HT29, DLD1, HCT116, HCT15 and LoVo were purchased from the American Type Culture Collection (ATCC; Manassas, VA, USA), and were cultured in RPMI-1640 medium containing 10% inactivated fetal bovine serum (FBS) and 1% antibiotics (penicillin and streptomycin) in 5% CO_2 at 37˚C. The non-transformed colonic epithelial NCM460 cells were obtained from INCELL Corporation (San Antonio, TX, USA) and cultured in M3 media supplemented with 10% FBS and 1% antibiotics (penicillin and streptomycin) in 5% CO_2 at 37˚C. Cells were sub-cultured at a seeding density of $1x10^6$ cells/ml, and allowed to grow to ~80% confluence for metabolic and lipidomic profiling experiments. HT29, SW620, SW480 and NCM460 cells are MMR proficient, whereas HCT116, LoVo, HCT15, DLD1 cells are MMR deficient. HCT116 cells lack MLH1 (12), whereas LoVo cells are deficient in MSH2 and MSH6 genes (13,14); HCT15 and DLD1 cells also lack the MSH6 protein (15). All experiments were performed in accordance with relevant guidelines and regulations.

Western blotting. Western blotting was performed to evaluate the protein expression levels of the MLH1, MSH2, MLH6 and PMS2 in the CRC cells and normal colonic mucosa cells. Briefly, the cells were harvested by centrifugation at 200 x g for 3 min, washed twice with ice-cold phosphate-buffered saline (PBS), and lysed with RIPA buffer with protease inhibitor cocktails. The concentrations of the protein extracts were assessed using the Coomassie brilliant blue G-250 method and equalized before loading. A total of 20 μg protein from each sample were separated on sodium dodecyl sulfate-polyacrylamide gel electrophoresis (10% SDS-PAGE) gels, and then transferred to polyvinylidene difluoride (PVDF) membranes. The membranes were blocked with 5% skim milk and incubated with specific primary antibodies overnight at 4˚C. After the incubation with the relevant secondary antibodies, the reactive bands were identified using an enhanced chemiluminescence kit (Amersham Biosciences, Piscataway, NJ, USA). The relative quantities of each protein were analyzed by probing the membranes with MLH1 (cat. no. 4256s), MSH2 (cat. no. 2017s), MLH6 (cat. no. 5424s) and PMS2 (cat. no. 2455s) antibodies (dilution 1:1,000; all were obtained from Cell Signaling Technology; New England BioLabs Ltd., Hertfordshire, UK) and using Gel-Pro Analyzer software. Data presented are from one representative experiment from 3 repeated experiments.

Reverse transcription polymerase chain reaction (RT-PCR). Total RNA was extracted from the cell lines using TRIzol reagent (Invitrogen; Thermo Fisher Scientific, Inc., Waltham, MA, USA), according to the manufacturer's protocol. cDNAs were synthesized using a Thermo-Scientific reverse transcription kit. Real-time PCR was conducted using the SsoAdvanced™ Universal SYBR-Green kit, according to the manufacturer's instructions: 95˚C pre-denaturation for 30 sec, 40 cycles at 95˚C denaturation for 5 sec, 60˚C refolding, and extension for 20 sec, followed by a dissolution curve analysis (65-95˚C in increments of 0.5˚C each 2-5 sec). Data represent the mean ± SEM from 3 repeated experiments with n=3.

Preparation of cell samples. Cells were placed on ice and washed with 1 ml of ice-cold PBS to remove extracellular metabolites. Cells were then detached using a cell scraper, and all cells were resuspended in PBS and centrifuged at 300 x g for 3 min. The culture mediums were aspirated, and the cells were suspended in PBS and transferred into 1.5 ml (Eppendorf) EP tubes.

Lipid extraction. Samples were extracted using a modified Folch procedure (16). Briefly, ice-cold chloroform (1 ml) and methanol (0.5 ml), with 0.1% butylated hydroxytoluene (BHT) were added to the dried cells and vortexed for 20 sec. The mixture was sonicated in a 4˚C water bath for 30 min and incubated on ice for 60 min with shaking. Phase separation was induced by the addition of 380 μl of water with 0.1% BHT, followed by incubation on ice for 10 min with shaking. The mixture was centrifuged at 18,500 x g for 10 min at 4˚C. The mixture was split into two aliquots, the lower (chloroform) phase was reserved for lipid analysis using nanoelectrospray ionization LC-MS. The extracts were passed through a 0.2-μm filter (Whatman, Maidstone, UK) and evaporated with nitrogen gas. The dried chloroform fraction was resuspended in 100 μl of methanol-chloroform (9:1, v/v) containing a 7.5-mM ammonium acetate buffer solution for analysis, and the dried methanol fraction was used in the derivatization procedures. All extracts were stored at -80˚C until use.

LC-MS lipid metabolite analysis. The UPLC-MS/MS portion of the platform was based on the ACQUITY Ultra High-Performance LC mass spectrometry system (Waters Corp., Milford MA, USA), and samples were analyzed using an electrospray ionization (ESI)-Q-TOF(quadrupole-time-of-flight) mass analyzer. The dried samples were redissolved in acetonitrile/isopropanol (v/v, 7:3), and the injection volume was fixed at 3 μl. One aliquot was analyzed using acidic-positive ion-optimized conditions, and the other was analyzed using basic negative ion-optimized conditions in two independent injections with separate dedicated columns (1.8 μm, 2.1x100 mm; Waters Corp.). The column was maintained at 45 to 55˚C. The flow rate of the mobile phase was 250 μl/min, and the injection volume was 5.0 μl Mobile phase A which consisted of acetonitrile/water at a 4/6 ratio (10 mmol ammonium acetate). Mobile phase B consisted of acetonitrile/isopropanol at a 1/9 ratio (10 mmol ammonium acetate). Extracts reconstituted in acid were eluted using a gradient of water and methanol containing 0.1% formic acid, and the basic extracts, which also used the water/methanol solvent, contained 6.5 mM ammonium bicarbonate. The MS analysis alternated between MS and data-dependent MS/MS scans using dynamic exclusion, and the scan range was 65-1,000 mass-to-charge ratios (m/z). All types of gas used nitrogen.

Full-scan spectra were collected at m/z values ranging from 50-1,200 for positive and negative ion modes. The mass spectra of each sample were acquired in profile mode over a 2-min period. The capillary temperature was set to 200˚C. The capillary and tube-lens voltages were set to 32 and 95 V, respectively, in positive ion mode and to -41 and -93 V in negative ion mode. The target automatic gain control values for full MS and multistage MS were 30,000 and 1,000, respectively. MS/MS was applied to pooled samples to identify lipid species. The normalized collision energy was set to 35%, with an isolated width of 1.5 m/z units and a charge state of 1. The dynamic exclusion parameters were a repeat duration of 60 sec, exclusion duration of 60 sec, and an exclusion list size of 50. Data represented the mean ± SEM from 3 repeated experiments with n=3.

Data processing and statistical analysis. UPLC-ESI-TOFMS data were processed using Progenesis QI software (Waters Corp., Newcastle, UK). Metabolites were identified by referring to the Lipid Maps Database (www.lipidmaps.org) and the Human Metabolome Database (http://www.hmdb.ca/). Data sheets were obtained from Progenesis QI software, and the absolute intensities of all identified compounds were recalculated to the relative abundances of lipid molecules. The resulting datasets from the positive and negative ion modes were further combined into one dataset prior to the statistical analysis. A partial least-square discriminant analysis (PLS-DA) was performed to evaluate differences between dMMR and pMMR colon cancer cell lines. The highest impact on group clustering was identified in the variable importance (VIP) plots (VIP >1). The expression of PLD1, lipin 1, SCD1 and DGAT1 was compared among the 8 cell lines with one-way analysis of variance (ANOVA) followed by Newman-Keuls post hoc test. Additionally, an unpaired Student's t-test (P<0.05) was applied to the chemical shifts and used to assess the significance of differences in each metabolite. The metabolites in two groups that exhibited both a VIP >1 and P<0.05 were identified as significantly different. Data are presented as the means ± SEM. Statistical analyses were performed using SPSS software (version 16.0; SPSS, Inc., Chicago, IL, USA).

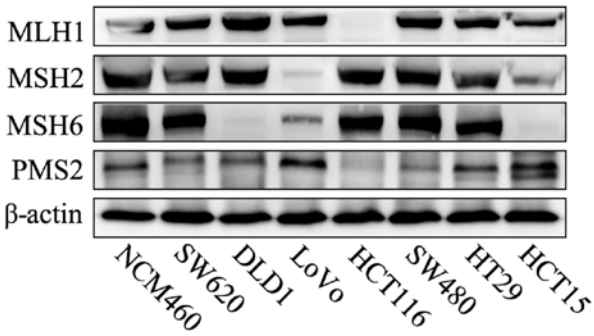

Figure 1. Western blot analysis of the MMR protein in CRC cell lines. NCM460, SW620, SW480 and HT29 were pMMR cells, and they expressed MLH1, PMS2, MSH2 and MSH6. In contrast, HCT116, LoVo, DLD1 and HCT15 were dMMR cells: HCT116 was deficient in MLH1 and PMS2, LoVo was deficient in MSH2 and MSH6, and both DLD1 and HCT15 were deficient in MSH6. MMR, DNA mismatch repair; CRC, colorectal cancer; pMMR, patients proficient in DNA MMR; dMMR, patients deficient in DNA MMR.

Results

Protein expression of MMR of the 8 cell lines. The 8 cell lines were examined by western blotting to assess the protein levels of MMR. The western blot analysis confirmed the HCT116 cells were deficient in MLH1 gene, LoVo cells were deficient in MSH2/MSH6 and DLD1 and HCT15 cells were deficient in MSH6. Thus, HCT116, LoVo, HCT15 and DLD1 were dMMR cells. In contrast, the presence of all 4 MMR proteins in SW620, SW480, HT29 and NCM460 indicated that all the 4 cell lines were pMMR CRC cells (Fig. 1). Therefore, the aforementioned 8 cell lines were divided into dMMR and pMMR cells in the subsequent experiments.

Comparative lipidomic and metabolic profiling of dMMR and pMMR cells. The lipidomic profiles significantly differed between dMMR and pMMR CRC cells. We detected a diverse range of lipid species to obtain models that enabled the discrimination of the 2 different cell types and identified potential biomarkers for dMMR and pMMR CRC cells. The LC-MS/MS lipidomic profiling of dMMR and pMMR cells detected 157 lipid molecules in 19 lipid classes, included phospholipids (85 molecules), sphingolipids (11 molecules), and glycerolipids (61 molecules) (Table I). A total of 157 lipids are displayed in the heat maps of the dMMR and pMMR cells showing the fold changes in altered lipids in dMMR cells compared with those in pMMR cells. The lipidome presented numerous and obvious alterations in multiple lipid classes (Fig. 2), including glycerolipids (GL), glycerophospholipids (GP) and sphingolipids (SP), suggesting that these 3 types of lipid species exhibit different biological behaviors in the dMMR and pMMR cells.

Table I. Quantitated lipid classes and numbers in dMMR and pMMR colorectal cancer cells.

Lipid category	Lipid class	Abbreviation	No. of lipid species
Phospholipid	Phosphatidylcholine	PC	27
	Alkylphosphatidylcholine	PC(O)	9
	Alkenylphosphatidylcholine	PC(P)	5
	Phosphatidylethanolamine	PE	18
	Alkylphosphatidylethanolamine	PE(O)	3
	Phosphatidylinositol	PI	3
	Phosphatidylserine	PS	1
	Alkylphosphatidylserine	PS(O)	4
	Alkenylphosphatidylserine	PS(P)	3
	Phosphatidylglycerol	PG	8
	Phosphatidic acid	PA	4
Sphingolipid	Sphingomyelin	SM	5
	Ceramide	Cer	2
	Glycosylceramide	Gcer	1
	Lactosylceramide	Lcer	3
Glycerolipide	Monoacylglycerol	MG	3
	Diacylglycerol	DG	31
	Triacylglycerol	TG	27
Total lipids			157

dMMR, deficient in DNA MMR; pMMR, patients proficient in DNA MMR.

For all lipid classes, the masses of the lipid species altered in pMMR cells were much greater than those in dMMR cells. The two main lipid classes detected in dMMR and pMMR cells were phosphatidylcholine (PC) and phosphatidylethanolamine (PE) (Fig. 3A). Significantly higher levels (~2-fold) of the phosphatidylinositol (PI) class were detected in pMMR cells than those in dMMR cells, and a similar trend was observed in the phosphatidic acid (PA) (Fig. 3A). Ceramide (Cer), the center of the sphingolipid metabolism pathway, also exhibited the same trend (Fig. 3B). Cer levels were significantly decreased in dMMR cells. Furthermore, the levels of the downstream metabolites of Cer, including glucosylceramide (GlcCer) and galactosylceramide (LacCer), were markedly decreased in the dMMR cells (Fig. 3B).

We compared the composition of the lipidomes between the dMMR and pMMR cells, and the OPLS-DA score plot further revealed the obvious and distinctive metabolic clusters between these 2 groups. As shown in Fig. 3C, the predicted residual sum of square (PRESS) was 0.4018 in the positive ion mode, indicating that the metabolites exhibited an intrinsic clustering pattern. Thirty-six significantly distinguished lipids were observed in the two groups, which satisfied the requirements of a VIP >1, a fold change and $P \leq 0.05$ according to Student's t-test, which contributed to the characterization of differences between dMMR and pMMR cells, and the detailed information on their identification is listed in Table II. As shown in Fig. 3D, 10 types of lipids exhibited the most significant changes between dMMR and pMMR cells. These 10 lipids were PC (34:1), PC (32:1), Cer (32:0), Cer (36:0), Cer (34:1), PC (36:1), PC (36:0), PC (38:4), SM (34:1) and PE (36:4). The levels of PC (34:1), PC (36:0), PC (36:1), Cer (32:0), Cer (36:0), Cer (34:1) and PC (38:4) in pMMR CRC cells were significantly increased compared with those in dMMR cells, whereas the levels of PC (32:1) and SM (34:1) were significantly elevated in dMMR CRC cells compared with those in pMMR cells. The trends in the changes in the levels of these 10 lipids between the dMMR and pMMR CRC cells are shown in Fig. 3E. Notably, the levels of SPs [Cer (32:0), Cer (34:1)] and GPs [PC (34:1), PC (36:0), PC (36:1) and PC (38:4)] were significantly increased in pMMR cells compared with those in dMMR cells.

Verification of the relevance of the association of the mRNA expression levels of SCD1, SCD5, DGAT1, PAP and PLD1 with the invasion and metastasis of dMMR and pMMR cells. Since patients with pMMR are more likely to have metastases and a higher level of PC, PA, and ceramide than those with dMMR, and lipid metabolism plays a pivotal role in cancer metastasis (17), we subsequently investigated the change of key enzymes involved in lipid metabolism associated with metastasis, which are stearoyl-CoA desaturases (SCD1), diacylglycerol acyltransferase 1 (DGAT1), lipin 1 and phospholipase D (PLD), for the mRNA analysis of RT-PCR (17). The expression levels of SCD1, DGAT1, lipin 1 and PLD1 in 7 different CRC cell lines and intestinal mucosa cells were detected using RT-PCR. SCD1 is closely related to the stage, grade and lymph node metastasis of renal cell carcinoma, and SCD1 suppression could make cancer patients more sensitive to various therapies (18). As shown in Fig. 4, significantly increased levels of SCD1 were detected in HT29 and SW620 cells compared with those in LoVo, DLD1 and HCT15 cells. Diacylglycerol

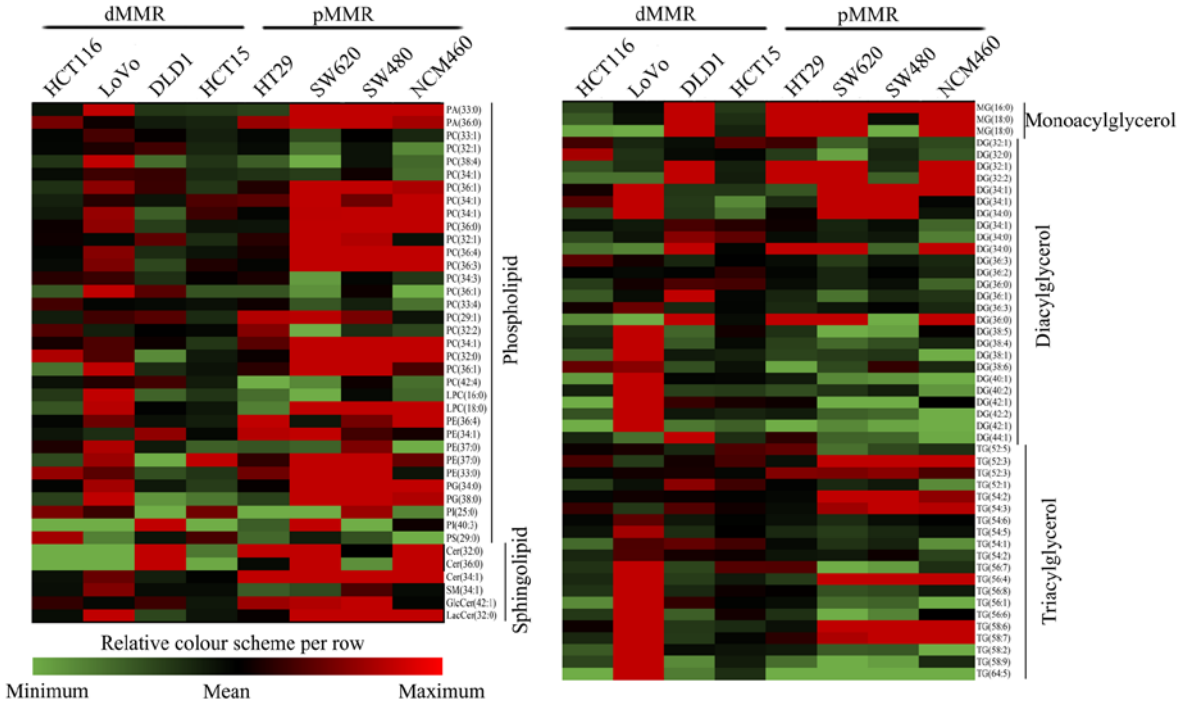

Figure 2. Comparative lipid profile expression in dMMR and pMMR cells. The heat maps revealed all modified lipid species in dMMR and pMMR cells. The color bars represent the log2 value of the ratio for each lipid species and only statistically significant changes are shown (VIP >1, P<0.05). Statistical analysis for individual lipid species data were based on the unpaired two-tailed Student's t-test. PA, phosphatidic acid; PC, phosphatidylcholine; PE, phosphatidylethanolamine; PG, phosphatidylglycerol; PI, phosphatidylinositol; PS, phosphatidylserine. LPC, lysophosphatidylcholine; MG, monoacylglycerol; DG, diacylglycerol; TG, triacylglycerol; Cer, ceramide; SM, sphingomyelin; GlcCer, glucosylceramide; LacCer, lactosylceramide; pMMR, patients proficient in DNA MMR; dMMR, patients deficient in DNA MMR.

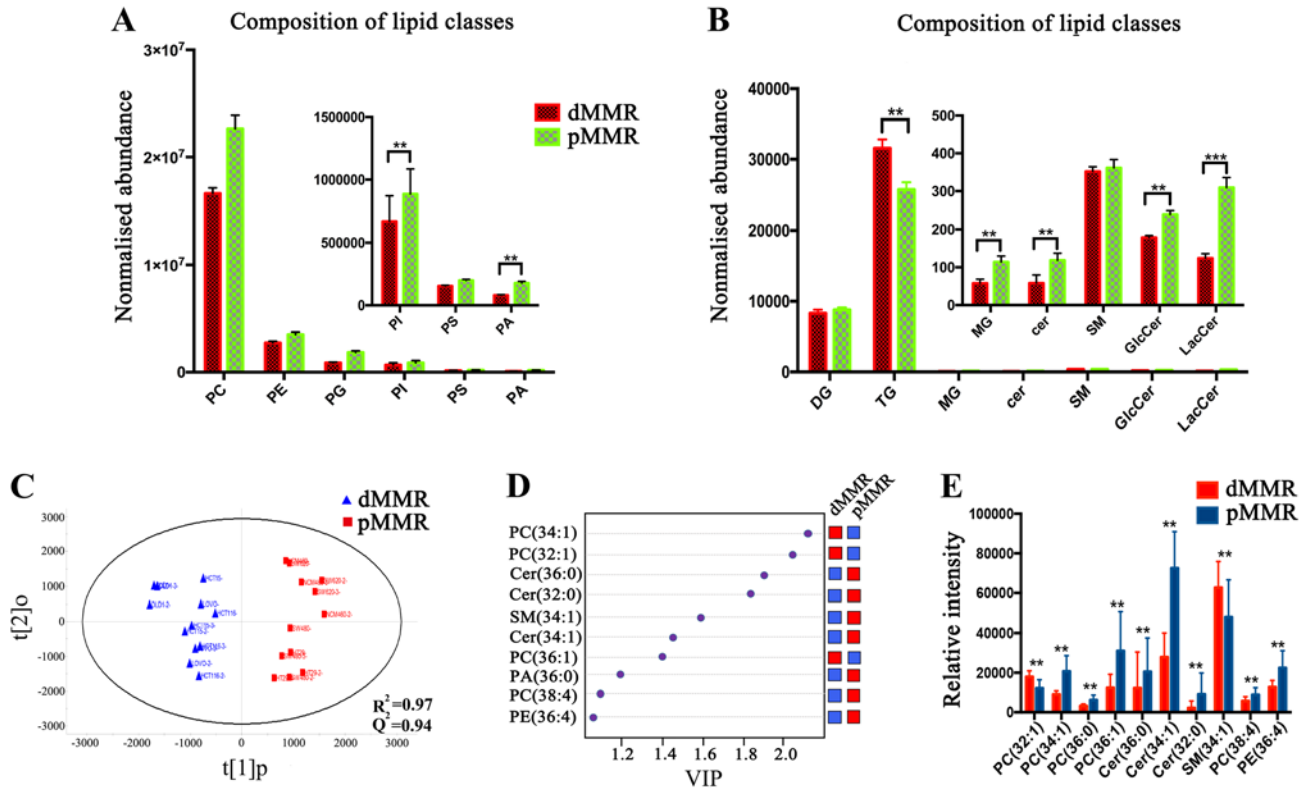

Figure 3. Comparative lipidomic metabolic profiling of dMMR and pMMR cells. (A and B) Lipid class comparison between the dMMR and pMMR groups. The two main lipid classes detected were phosphatidylcholine (PC) and phosphatidylethanolamine (PE), and the change of lipids in pMMR cells was more obvious than dMMR cells. (C) The OPLS-DA score plot for the top two components discriminating dMMR and pMMR cells were detected by UPLC-MS under the positive ionization mode; red points represent pMMR cells and blue squares represent dMMR cells. (D) Ten common variables labeled had significant differences in their levels between the dMMR and pMMR cells. (E) Change trends of these 10 lipids in the dMMR (red bar) and the pMMR cells (blue bar). (**P<0.01; ***P<0.001). pMMR, patients proficient in DNA MMR; dMMR, patients deficient in DNA MMR.

Table II. Identification of significantly altered lipid species from dMMR and pMMR cells, along with P-values and relative changes.

Ion mode	Ion form	Metabolite	Molecular formula	M/Z	P-value	Fold change	VIP
(+)	$[M+H]^+$	PA(36:1)	C39H75O7P	709.5140275	2.16E-06	1.84	1.84
(+)	$[M+H]^+$	PC(32:0)	C40H82NO7P	720.5904492	0.0009	2.01	1.87
(+)	$[M+H]^+$	PC(32:1)	C40H80NO7P	718.5711243	0.0135	1.56	1.68
(+)	$[M+H]^+$	PC(32:2)	C40H76NO8P	730.5384427	0.0344	1.32	1.39
(+)	$[M+H]^+$	PC(34:1)	C42H84NO7P	746.6058638	9.20E-06	2.29	1.97
(+)	$[M+H]^+$	PC(34:2)	C42H82NO7P	744.5898594	7.20E-05	1.68	1.63
(+)	$[M+H]^+$	PC(34:3)	C42H78NO8P	778.5360776	0.0323	1.30	1.4
(+)	$[M+H]^+$	PC(36:0)	C44H88NO8P	772.6191553	0.0004	1.94	1.76
(+)	$[M+H]^+$	PC(36:1)	C44H88NO7P	774.6343973	0.0019	2.49	1.73
(+)	$[M+H]^+$	PC(36:3)	C44H84NO7P	792.5829337	9.20E-05	2.18	1.49
(+)	$[M+H]^+$	PC(36:4)	C44H82NO7P	790.568157	3.26E-05	1.89	1.33
(+)	$[M+H]^+$	PC(38:4)	C46H84NO8P	832.5822233	0.0231	1.81	1
(+)	$[M+H]^+$	PC(34:1)	C42H82NO7P	766.5693969	0.0014	1.71	1.32
(+)	$[M+H]^+$	PC(32:1)	C40H78NO8P	732.5557817	0.0017	1.47	1.39
(+)	$[M+H]^+$	PC(34:1)	C42H82NO8P	760.5882343	0.0028	1.37	1.85
(+)	$[M+H]^+$	LysoPC(16:0)	C24H50NO7P	496.3394888	0.0207	1.81	1.23
(+)	$[M+H]^+$	LysoPC(18:0)	C26H54NO6P	508.3755192	0.0124	3.20	1.12
(+)	$[M+H]^+$	PE(34:1)	C39H76NO8P	740.5532847	0.0028	1.55	1.26
(+)	$[M+H]^+$	PE(36:4)	C41H74NO7P	724.5283148	0.0037	1.48	1.36
(+)	$[M+H]^+$	PE(32:1)	C37H72NO8P	690.5339367	0.0082	1.34	1.34
(+)	$[M+H]^+$	PG(34:0)	C40H79O10P	768.5763566	8.27E-05	2.13	1.72
(+)	$[M+H]^+$	PG(38:0)	C44H87O10P	824.6407199	0.0083	1.99	1.89
(+)	$[M+H]^+$	SM(34:2)	C39H77N2O6P	701.5585441	0.0229	1.30	1.81
(+)	$[M+H]^+$	Cer(32:0)	C32H65NO3	529.5294728	0.0368	4.05	1.21
(+)	$[M+H]^+$	Cer(36:0)	C36H73NO3	590.5496807	0.0172	1.68	1.02
(+)	$[M+H]^+$	LacCer(32:0)	C44H85NO13	818.6013832	8.96E-05	2.60	1.41
(-)	$[M+H]^-$	PC(36:0)	C44H88NO7P	754.6076572	0.0295	1.21	1.7
(-)	$[M+H]^-$	PC(38:2)	C46H88NO8P	858.6227992	0.0145	1.55	1.14
(-)	$[M+H]^-$	PC(38:4)	C46H86NO7P	776.5934588	0.0021	1.77	1.93
(-)	$[M+H]^-$	PA(38:2)	C41H67O8P	763.4559916	0.0427	17.79	1.03
(-)	$[M+H]^-$	PS(38:0)	C44H88NO9P	804.6133866	0.0120	1.31	1.73
(-)	$[M+H]^-$	PE(36:3)	C45H84NO7P	780.5900251	0.0195	1.35	1.04
(-)	$[M+H]^-$	SM(34:1)	C39H79N2O6P	747.564329	0.0290	1.51	1.08
(-)	$[M+H]^-$	SM(40:2)	C45H90N2O6P+	784.6425057	0.0134	2.00	1.23
(-)	$[M+H]^-$	LacCer(34:1)	C46H87NO13	906.6192601	0.0057	1.55	1.46
(-)	$[M+H]^-$	LacCer(36:2)	C48H89NO13	886.6217938	0.0137	1.34	1.05

dMMR, deficient in DNA MMR; pMMR, patients proficient in DNA MMR. PA, phosphatidic acid; PC, phosphatidylcholine; PE, phosphatidylethanolamine; PG, phosphatidylglycerol; PS, phosphatidylserine. LysoPC, lysophosphatidylcholine; Cer, ceramide; SM, sphingomyelin; GlcCer, glucosylceramide; LacCer, lactosylceramide.

acyltransferase 1 (DGAT1) is the enzyme at the final step in TG synthesis (Fig. 5). The overexpression of DGAT1 has been revealed to inhibit the growth and aggressiveness of tumor cells, and it is a negative regulator of malignant progression of the tumor (19). Notably, the level of DGAT1 expression was significantly increased in dMMR cells compared with that in pMMR cells, except for DLD1 cells (Fig. 4). PAP is coded by the lipin 1 gene, which is a negative regulator of the malignant progression of the tumor (20,21). The expression of lipin 1 in dMMR cells was higher than that in pMMR cells (Fig. 4). PLD1 has a direct effect on cell migration, and is a key enzyme involved in cell invasion and metastasis (19). PLD1 expression was higher in pMMR cells (HT29 and SW480 cells) than in dMMR cells (Fig. 4).

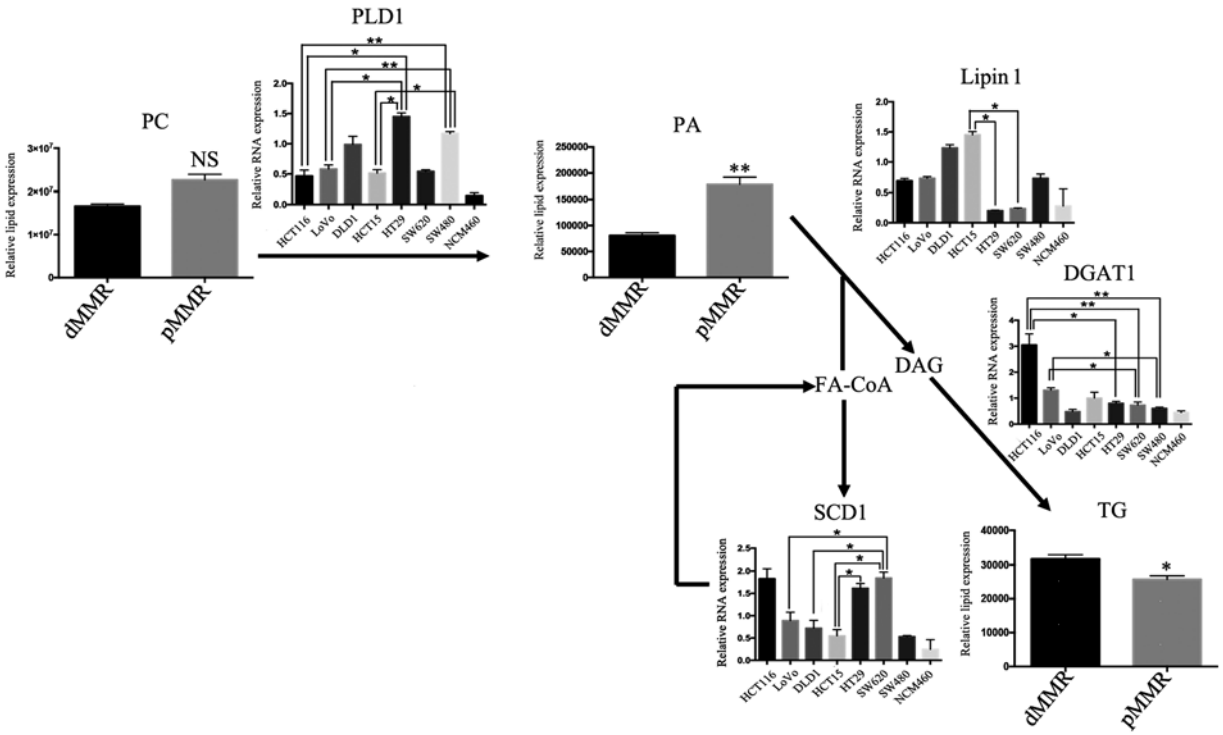

Figure 4. Levels of lipogenic invasion and metastasis gene mRNAs in lipid biosynthetic pathways. Levels of lipogenic gene mRNAs in the lipidomic network in dMMR and pMMR CRC cells. The gene with the highest invasion and metastasis was selected as the representative of each pathway. Data represent sums of ion peak heights of all lipid molecules within each class and are illustrated as the mean ± SD. The statistical significance of the differences between measurements in the dMMR and pMMR cells was assessed using a non-paired Student's t-test with FDR adjustment. The expression of PLD1, lipin 1, SCD1 and DGAT1 was compared among the 8 cell lines with one-way analysis of variance (ANOVA) followed by Newman-Keuls post hoc test. *P<0.05; **P<0.01; NS, not statistically significant. Abbreviations are described in Table I. The PLD1, PLD2, lipin 1, DGAT1, and SCD1 genes with the highest invasion and metastasis, and the expression in 8 cell lines by RT-PCR. PLD hydrolyzes PC to produce PA. DGAT is a key enzyme involved in the formation of TG by DAG and FA-CoA. The dephosphorylation of PA could form DAG, which represents one of the steps in TG synthesis. SCD is an important enzyme involved in the synthesis of FAs. PA, phosphatidic acid; PC, phosphatidylcholine; PE, phosphatidylethanolamine; PG, phosphatidylglycerol; PI, phosphatidylinositol; PS, phosphatidylserine. LPC, lysophosphatidylcholine; MG, monoacylglycerol; DG, diacylglycerol; TG, triacylglycerol; Cer, ceramide; SM, sphingomyelin; GlcCer, glucosylceramide; LacCer, lactosylceramide; pMMR, patients proficient in DNA MMR; dMMR, deficient in DNA MMR.

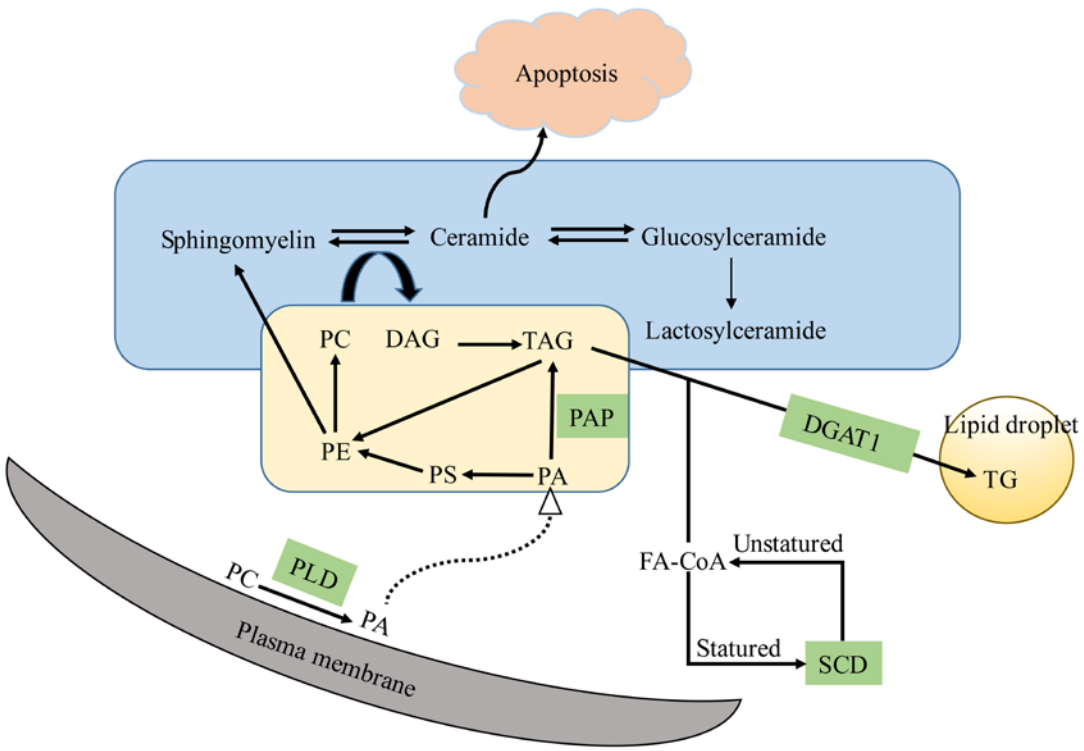

Figure 5. The lipid integrative metabolic network, which is involved in lipid metabolism and interconnection of metastasis and invasion.

Discussion

With improvement of molecular biological techniques, detecting MMR genes has become relatively simple and accurate. MMR plays an important role in the development and progression of CRC, and the detection of MMR genes is of great significance in the prevention, early diagnosis and treatment of CRC (7,20). Compared to dMMR patients, pMMR patients have early metastases and poor prognosis. Lipid metabolism plays an important role in tumor invasion and metastasis, and alterations in the metabolic program are crucial in cancer metastasis (5). However, the impact of the lipidome on MMR is largely unknown. In this study, MMR lipid metabolites were detected using UPLC-MS, and the differences in the levels of lipid metabolites were also screened. This is the first study to analyze the difference of lipid metabolic profiles between dMMR and pMMR cells. According to the OPLS-DA score plot, a VIP >1 and P<0.05 were obtained for 157 different metabolites, which was used to differentiate human colon epithelial cells from dMMR and pMMR cells, suggesting two different categories of membrane lipid components. Forty-six significantly different metabolites were identified, and the levels of the main classes of GL, GP and SP metabolites were significantly higher in pMMR cells than dMMR cells.

The levels of membrane phospholipids, including PC, PE, PI, SM and Cer, were higher in cancer tissues than those in normal tissue samples, particularly in tumor tissues with higher invasiveness (20,21). Indeed, PC has been used as a marker of membrane proliferation in tumors or as a predictive biomarker for monitoring the tumor response (22). In our study, the levels of most phospholipids were higher in pMMR CRC cells than those in dMMR cells. These lipids (PS 18:0/20:4, PC 18:0/20:4) significantly increased the invasive ability of the pMMR cells, suggesting that they represent potential biomarkers for metastasis. Overexpression of fatty acid synthase plays an important role in tumorigenesis and *de novo* synthesis of fatty acids is required for the rapid proliferation of cancer cells (23).

As shown in Fig. 5, the enzymes associated with lipid metabolism play an important role in the change of membrane lipid levels in dMMR and pMMR cells. Lipid metabolism plays an important role in the development of cancer, since lipid metabolism is regulated to satisfy the increasing energy needs (17). Therefore, the primary tumor transfers to the metastatic site through the actions of a number of metabolic enzymes. The prognosis of CRC patients with pMMR is better than CRC patients with dMMR, which is associated with less invasion and distant metastasis in CRC patients with dMMR, and SCD, PAP, PLD and DGAT1 are associated with tumor invasion and metastasis (17). In our study, pMMR cells (HT29 and SW620 cells) were found to express a higher level of PLD but a lower level of DGAT1, and pMMR cells (HT29 and SW480 cells) were also found to express a higher level of SCD1. Through the study of different enzymes involved in lipid metabolism, we may identify potential anti-metastasis targets in the therapy of patients with pMMR.

In this study, the PLS regression model was successfully used to distinguish between dMMR and pMMR cells with high predictive accuracy. Lipidomic and metabolic methods offer an in-depth understanding of the alterations in metabolism of CRC. This study also supplied valuable new information related to CRC divided into dMMR and pMMR types and applied a completely different in-depth strategy to identify the most suitable treatment strategies for patients with dMMR and pMMR CRCs in the area of standardized treatment based on the development of individualized treatment programs and the development of potential therapeutic drugs. The underlying mechanisms of MMR genes in tumor cells, such as the apoptosis-related mechanism, are still unclear. Researchers have not clearly determined whether other genes located upstream and downstream of the MMR pathway may represent new therapeutic targets. DNA MMR genes are neither oncogenes nor tumor-suppressor genes. Further research is warranted to understand the relationship between the DNA MMR genes and oncogene/tumor-suppressor genes and to determine why patients with pMMR CRC are resistant to chemotherapeutic drugs and other treatments.

In conclusion, in the present study, we used a lipidomics profiling experiment to analyze the difference in lipid metabolism between dMMR and pMMR cells. Our data revealed that 10 types of lipids exhibited the most significant changes between dMMR and pMMR cells. Thus, elucidating the molecular basis of the alterations in these genes is important to better understand the differences in the pathophysiology of dMMR and pMMR CRC patients, identify different MMR gene deletions to develop a better treatment plan for patients, and identify potential therapeutic targets. To the best of our knowledge, we are the first to reveal that the levels of metastasis- associated lipids and key enzymes in lipid metabolism are found to be higher in the CRC patients with pMMR compared with the CRC patients with dMMR. Our discovery provided the identification of potential anti-metastasis targets in the therapy of patients with pMMR, and also personalized therapy for patients with pMMR.

Acknowledgements

Not applicable.

Funding

The present study was supported by grants from the Qian Ke He LH (2016) 7195 and Qian Ke He JC (2016) 1094.

Availability of data and materials

The datasets used during the present study are available from the corresponding author upon reasonable request.

Authors' contributions

WP, YLZ and QL conceived and designed the study. WP, SST, YZX, LW, DQ, CC, YYL, CQL, ZLL and YL performed the experiments. WP wrote the manuscript. WP, YLZ, and QL reviewed and edited the manuscript. All authors read and approved the manuscript and agree to be accountable for all aspects of the research in ensuring that the accuracy or integrity of any part of the work are appropriately investigated and resolved.

Ethics approval and consent to participate

Not applicable. This study does not contain any studies with human participants or animals performed by any of the authors.

Patient consent for publication

Not applicable.

Competing interests

The authors declare that they have no competing interests.

References

1. Siegel RL, Miller KD and Jemal A: Cancer Statistics, 2017. CA Cancer J Clin 67: 7-30, 2017.
2. Bockelman C and Glimelius B: Need for adjuvant chemotherapy after colon cancer surgery-has it decreased? Acta Oncol 56: 629-633, 2017.
3. Hewish M, Lord CJ, Martin SA, Cunningham D and Ashworth A: Mismatch repair deficient colorectal cancer in the era of personalized treatment. Nat Rev Clin Oncol 7: 197-208, 2010.
4. Lee K, Tosti E and Edelmann W: Mouse models of DNA mismatch repair in cancer research. DNA Repair 38: 140-146, 2016.
5. Kawakami H, Zaanan A and Sinicrope FA: Microsatellite instability testing and its role in the management of colorectal cancer. Curr Treat Options Oncol 16: 30, 2015.
6. Tejpar S, Saridaki Z, Delorenzi M, Bosman F and Roth AD: Microsatellite instability, prognosis and drug sensitivity of stage II and III colorectal cancer: More complexity to the puzzle. J Natl Cancer Inst 103: 841-844, 2011.
7. Supek F and Lehner B: Differential DNA mismatch repair underlies mutation rate variation across the human genome. Nature 521: 81-84, 2015.
8. Ray U and Roy SS: Aberrant lipid metabolism in cancer cells-the role of oncolipid-activated signaling. FEBS J 285: 432-443, 2018.
9. Beloribi-Djefaflia S, Vasseur S and Guillaumond F: Lipid metabolic reprogramming in cancer cells. Oncogenesis 5: e189, 2016.
10. Wenk MR: Lipidomics: New tools and applications. Cell 143: 888-895, 2010.
11. Deng L, Gu H, Zhu J, Nagana Gowda GA, Djukovic D, Chiorean EG and Raftery D: Combining NMR and LC/MS Using Backward Variable Elimination: Metabolomics Analysis of Colorectal Cancer, Polyps, and Healthy Controls. Anal Chem 88: 7975-7983, 2016.
12. Cannavo E, Marra G, Sabates-Bellver J, Menigatti M, Lipkin SM, Fischer F, Cejka P and Jiricny J: Expression of the MutL homologue hMLH3 in human cells and its role in DNA mismatch repair. Cancer Res 65: 10759-10766, 2005.
13. Drummond JT, Genschel J, Wolf E and Modrich P: *DHFR/MSH3* amplification in methotrexate-resistant cells alters the hMutSalpha/hMutSbeta ratio and reduces the efficiency of base-base mismatch repair. Proc Natl Acad Sci USA 94: 10144-10149, 1997.
14. Kantelinen J, Kansikas M, Korhonen MK, Ollila S, Heinimann K, Kariola R and Nyström M: MutSbeta exceeds MutSalpha in dinucleotide loop repair. Br J Cancer 102: 1068-1073, 2010.
15. Umar A, Koi M, Risinger JI, Glaab WE, Tindall KR, Kolodner RD, Boland CR, Barrett JC and Kunkel TA: Correction of hypermutability, *N*-methyl-*N*'-nitro-N-nitrosoguanidine resistance, and defective DNA mismatch repair by introducing chromosome 2 into human tumor cells with mutations in *MSH2* and *MSH61*. Cancer Res 57: 3949-3955, 1997.
16. Folch J, Lees M and Sloane stanley GH: A simple method for the isolation and purification of total lipides from animal tissues. J Biol Chem 226: 497-509, 1957.
17. Luo X, Cheng C, Tan Z, Li N, Tang M, Yang L and Cao Y: Emerging roles of lipid metabolism in cancer metastasis. Mol Cancer 16: 76, 2017.
18. Wang H, Zhang Y, Lu Y, Song J, Huang M, Zhang J and Huang Y: The role of stearoyl-coenzyme A desaturase 1 in clear cell renal cell carcinoma. Tumour Biol 37: 479-489, 2016.
19. Bagnato C and Igal RA: Overexpression of diacylglycerol acyltransferase-1 reduces phospholipid synthesis, proliferation, and invasiveness in simian virus 40-transformed human lung fibroblasts. J Biol Chem 278: 52203-52211, 2003.
20. Kim HY, Lee KM, Kim SH, Kwon YJ, Chun YJ and Choi HK: Comparative metabolic and lipidomic profiling of human breast cancer cells with different metastatic potentials. Oncotarget 7: 67111-67128, 2016.
21. Hilvo M, Denkert C, Lehtinen L, Muller B, Brockmoller S, Seppänen-Laakso T, Budczies J, Bucher E, Yetukuri L, Castillo S, *et al*: Novel theranostic opportunities offered by characterization of altered membrane lipid metabolism in breast cancer progression. Cancer Res 71: 3236-3245, 2011.
22. Iorio E, Ricci A, Bagnoli M, Pisanu ME, Castellano G, Di Vito M and Venturini E, Glunde K, Bhujwalla ZM, Mezzanzanica D, Canevari S and Podo F: Activation of phosphatidylcholine cycle enzymes in human epithelial ovarian cancer cells. Cancer Res 70: 2126-2135, 2010.
23. Menendez JA and Lupu R: Fatty acid synthase and the lipogenic phenotype in cancer pathogenesis. Nat Rev Cancer 7: 763-777, 2007.